

Finite-size and pressure effects in $\text{YBa}_2\text{Cu}_4\text{O}_8$ probed by magnetic field penetration depth measurements

R. Khasanov,^{1,2,*} T. Schneider,¹ J. Karpinski,³ and H. Keller¹

¹*Physik-Institut der Universität Zürich, Winterthurerstrasse 190, CH-8057, Switzerland*

²*Laboratory for Muon Spin Spectroscopy, Paul Scherrer Institut, CH-5232 Villigen PSI, Switzerland*

³*Solid State Physics Laboratory, ETH 8093 Zürich, Switzerland*

We explore the combined pressure and finite-size effects on the in-plane penetration depth λ_{ab} in $\text{YBa}_2\text{Cu}_4\text{O}_8$. Even though this cuprate is stoichiometric the finite-size scaling analysis of $1/\lambda_{ab}^2(T)$ uncovers the granular nature and reveals domains with nanoscale size L_c along the c -axis. L_c ranges from 33.2 Å to 28.9 Å at pressures from 0.5 to 11.5 kbar. These observations raise serious doubts on the existence of a phase coherent macroscopic superconducting state in cuprate superconductors.

PACS numbers: 74.72.Bk, 74.62.Fj, 74.25.Ha, 83.80.Fg

I. INTRODUCTION

Since the discovery of superconductivity in cuprates by Bednorz and Müller¹ a tremendous amount of work has been devoted to their characterization. Indeed, the issue of inhomogeneities and their characterization is essential for applications and the interpretation of experimental data. Furthermore, there is even increasing evidence that inhomogeneities are an intrinsic property of cuprates.^{2,3,4,5,6,7,8} Studies of different cuprate families revealed the segregation of the material in superconducting and non-superconducting regions. In particular, neutron scattering experiments provide evidence for nanoscale cluster formation and percolative superconductivity in various cuprates.^{2,3} Electron paramagnetic resonance (EPR) studies reveal nanoscale phase separation in superconducting and dielectric regions of $\text{YBa}_2\text{Cu}_3\text{O}_{7-\delta}$ with $0.15 \leq \delta \leq 0.5$.⁴ Nanoscale spatial variations in the electronic characteristics have also been observed in underdoped $\text{Bi}_2\text{Sr}_2\text{CaCu}_2\text{O}_{8+\delta}$ with scanning tunnelling microscopy (STM),^{5,6,7,8} while x-ray diffraction in oxygen doped La_2CuO_4 single crystals⁹ provide evidence for superconducting domains with spatial extent $L_{ab} \approx 300$ Å in the ab -plane. Accordingly, there is considerable evidence for granular superconductivity in the cuprates. Although crystals of the cuprates are not granular in a structural sense, it occurs when microscopic superconducting domains are separated by non-superconducting regions through which they communicate for instance by Josephson tunnelling to establish the macroscopic superconducting state.

On the other hand, there is evidence for nearly isolated, homogeneous and superconducting domains of nanoscale extent embedded in a non-superconducting matrix.^{10,11,12,13} It stems from a finite-size scaling analysis of the thermal fluctuation contributions to the specific heat¹⁰ and magnetic penetration depth data.^{11,12,13} In an isolated domain there is a finite-size effect because the correlation length cannot grow beyond the length of the superconducting domain in direction i . Accordingly there is no sharp phase transition and the specific heat coefficient will exhibit a blurred peak with a maxi-

mum at $T_p < T_c$, where T_c is the transition temperature of the homogeneous bulk system. At T_p the correlation length $\xi(T)$ reaches the limiting length L of the domain. Similarly, $1/\lambda^2$, where λ is the magnetic field penetration depth, does not vanish at T_c , but exhibits a tail with an inflection point at T_p . This raises serious doubts on the existence of macroscopic phase coherent superconductivity, suggesting that bulk superconductivity is achieved by a percolative process. Therefore, superconducting properties and the spatial extent of the domains can be probed by thermal fluctuations and the finite-size effects. This includes the effects of oxygen isotope exchange and pressure on the domain size. Recently a significant change of spatial extent of the superconducting domains upon oxygen isotope exchange has been demonstrated in $\text{Y}_{1-x}\text{Pr}_x\text{Ba}_2\text{Cu}_3\text{O}_{7-\delta}$.¹¹ It revealed the relevance of local lattice distortions in occurrence of superconductivity.

This paper addresses the pressure studies of the finite-size effect in $\text{YBa}_2\text{Cu}_4\text{O}_8$, which exhibits a rather large and positive pressure effect (PE) on T_c , with $dT_c/dp = 0.59$ K/kbar.^{14,15,16} Even though this cuprate is *stoichiometric* the finite-size scaling analysis uncovers the existence of *nanoscale domains* with a spatial extent L_c along the crystallographic c -axis. The value of L_c decreases from 33.2 to 28.9 Å with increasing pressure from 0.5 to 11.5 kbar. Accordingly, T_c increases with *reduced thickness* L_c of the domains.

The paper is organized as follows. In Sec. II we sketch the finite-size scaling theory adapted for the analysis of penetration depth data. In Sec. III we describe sample preparation procedure and the experimental technique, adopted to deduce the in-plane magnetic field penetration depth λ_{ab} from the Meissner fraction measurements. In Sec. IV we perform the finite-size analysis of the data for the in-plane magnetic penetration depth $\lambda_{ab}(T)$ taken at different pressures. Sec. V comprises the analysis of the pressure dependence of the domain lengths L_c along the crystallographic c -axis.

II. THEORETICAL BACKGROUND

In a homogeneous bulk system, undergoing a fluctuation dominated continuous phase transition at T_c , the correlation length diverges as¹⁷

$$\xi(T) = \xi_0^\pm |T/T_c - 1|^{-\nu} = \xi_0^\pm |t|^{-\nu} \quad (1)$$

(\pm refers to $T > T_c$ and $T < T_c$, respectively, ξ_0^\pm is the critical amplitude and ν is the associated critical exponent). There is mounting evidence that in the experimentally accessible critical regime cuprates belong to the 3D-XY universality class (like superfluid He⁴) with $\nu \approx 2/3$.¹⁸ Since the order parameter Ψ is a complex scalar it corresponds to a vector with two components. For this reason below T_c there are two correlation lengths. The longitudinal one, ξ^l , is associated with the correlation function $\langle \text{Re}\Psi(R) \text{Re}\Psi(0) \rangle - \langle \text{Re}\Psi(0) \rangle^2$, while the transverse one, ξ^t , measures the decay of $\langle \text{Im}\Psi(R) \text{Im}\Psi(0) \rangle$. In the long wavelength limit considered here, the total correlation function is dominated by transverse fluctuations so that ξ^t is the relevant length scale.^{18,19} Suppose that the cuprates are granular, consisting of superconducting domains embedded in a non-superconducting matrix. Denoting the spatial extent of the domains along the crystallographic a , b and c -axis with L_a , L_b and L_c , the transverse correlation lengths ξ_i^t cannot diverge according to Eq. 1 but are limited by

$$\xi_i^t \xi_j^t \leq L_k^2, \quad i \neq j \neq k. \quad (2)$$

Consequently, for finite superconducting domains, the thermodynamic quantities, like the specific heat and penetration depth, are smooth functions of temperature. As a remnant of the singularity at T_c these quantities exhibit a so called finite-size effect,^{20,21} namely a maximum or an inflection point at T_{p_i}

$$\xi_i^t(T_{p_i}) \xi_j^t(T_{p_i}) = L_k^2, \quad i \neq j \neq k. \quad (3)$$

Close to criticality of the infinite system, the thermodynamic properties of its finite counterpart are well described by the finite-size scaling theory.^{20,21} In particular, the thermodynamic observable Q adopts the scaling form²²

$$\frac{Q(t, L)}{Q(t, L = \infty)} = f(x), \quad x = \frac{L}{\xi(t, L = \infty)}. \quad (4)$$

The scaling function f depends only on the dimensionless ratio $L/\xi(t, L = \infty)$ and does not depend on microscopic details of the system. It does, however, depend on the boundary conditions and the geometry of the system. As an example, for $Q(t, L) = \xi_i^t \xi_j^t$ we obtain from Eqs. (3) and (4) the finite-size scaling relation

$$\frac{\xi_i^t \xi_j^t}{\xi_{0i}^t \xi_{0j}^t} |t|^{2\nu} = f\left(\frac{\text{sign}(t)|t|^\nu L_k}{\sqrt{\xi_{0i}^t \xi_{0j}^t}}\right). \quad (5)$$

To relate this combination of transverse correlation lengths to an experimentally accessible quantity we invoke the universal relation^{18,23}

$$\frac{1}{\lambda_i^2(T)} = \frac{16\pi^3 k_B T}{\Phi_0^2 \xi_i^t(T)}, \quad (6)$$

which holds in the 3D-XY universality class (Φ_0 is the flux quantum, k_B is the Boltzmann's constant and λ_i is the London penetration depth). In this case the Eq. (5) reduces to

$$\frac{\lambda_{0i} \lambda_{0j}}{\lambda_i \lambda_j} |t|^{-\nu} = \left(\frac{\xi_i^t \xi_j^t}{\xi_{0i}^t \xi_{0j}^t}\right)^{-\frac{1}{2}} |t|^{-\nu} = g(y), \quad (7)$$

where y is equal to

$$y = \text{sign}(t) |t| \left(\frac{L_k}{\sqrt{\xi_{0i}^t \xi_{0j}^t}}\right)^{1/\nu} = \text{sign}(t) \left|\frac{t}{t_{p_k}}\right|$$

For the homogenous system ($L_k \rightarrow \infty$) and $t \neq 0$ ($y \neq 0$), $g(y)$ corresponds to the stepwise function

$$g_\infty(y < 0) = 1, \quad g_\infty(y > 0) = 0. \quad (8)$$

While for the system confined by the finite geometry ($L_k \neq 0$) the scaling function $g(y)$ diverges at $t \rightarrow 0$ ($y \rightarrow 0$) as

$$g(y \rightarrow 0) = g_{0k} y^{-\nu} = g_{0k} \left(\left|\frac{t}{t_{p_k}}\right|\right)^{-\nu}. \quad (9)$$

In order to obtain the absolute values of the inflection temperature T_{p_i} and the superconducting domain size L_i one can use the following procedure. Combining Eqs. (3) and (6) one obtains at the inflection point

$$\frac{1}{\lambda_i(T) \lambda_j(T)} \Big|_{T=T_{p_k}} = \frac{16\pi^3 k_B T_{p_k}}{\Phi_0^2} \frac{1}{L_k}. \quad (10)$$

For an infinite and homogeneous system $1/(\lambda_i(T) \lambda_j(T))$ decreases continuously with increasing temperature and vanishes at T_c , while for finite domains it does not vanish and exhibits an inflection point at $T_{p_k} < T_c$, so that

$$d\left(\frac{1}{\lambda_i(T) \lambda_j(T)}\right) / dT \Big|_{T=T_{p_k}} = \text{extremum} \quad (11)$$

Note, that in this paper we analyze experimental data for the temperature dependence of the in-plane penetration depth λ_{ab} taken at various applied pressures. In this case the domain size along c -axis (L_c) can be estimated according to Eq. (10) as

$$L_c = \frac{16\pi^3 k_B T_{p_c} (\lambda_a(T) \lambda_b(T))_{T=T_{p_c}}}{\Phi_0^2}, \quad (12)$$

that for $\lambda_a \simeq \lambda_b$ reduces to

$$L_c \simeq \frac{16\pi^3 k_B T_{pc} \lambda_{ab}^2 (T_{pc})}{\Phi_0^2}. \quad (13)$$

To summarize, the main signatures for the existence of finite-size behavior appearing in the temperature dependence of λ_{ab}^2 are:

- (i) The scaling function $g(y)$ diverges at $T = T_c$ ($t = 0$, $y = 0$) [Eq. (9)].
- (ii) $\lambda^{-2}(T)$ has an inflection point at $T_p < T_c$ [Eq.(10)].
- (iii) The first derivative of $\lambda^{-2}(T)$ at $T = T_p$ has an extremum [Eq.(11)].

III. EXPERIMENTAL DETAILS

A. Sample preparation and characterization

The polycrystalline $\text{YBa}_2\text{Cu}_4\text{O}_8$ samples were synthesized by solid-state reactions using high-purity Y_2O_3 , BaCO_3 and CuO . The samples were calcinated at 880 – 935 °C in air for 110 hours with several intermediate grindings. The phase-purity of the material was examined using a powder x-ray diffractometer. Only $\text{YBa}_2\text{Cu}_3\text{O}_{7-x}$ and CuO phases were revealed. The synthesis was continued at high oxygen pressure of 500 bar, at 1000 °C during 30 hours. The x-ray diffraction measurements performed after the final stage of the synthesis revealed 95 % of $\text{YBa}_2\text{Cu}_4\text{O}_8$ phase. The sample was then regrounded in a mortar for about 60 min in order to obtain sufficiently small grains, as required for the determination of λ from Meissner fraction measurements. The field-cooled (FC) magnetization (M) measurements were performed with a Quantum Design SQUID magnetometer in a field of 0.5 mT for temperatures ranging from 5 K to 100 K. The absence of weak links between grains has been confirmed by the linear magnetic field dependence of the FC magnetization, measured at 0.5 mT, 1 mT and 1.5 mT for each pressure at $T = 10$ K.

The hydrostatic pressure was generated in a copper-beryllium piston cylinder clamp that was especially designed for magnetization under pressure measurements (see Ref. [24]). The sample was mounted in a led container filled with Fluorient FC77 as a pressure transmitting medium with a sample to liquid volume ratio approximately 1/8. The pressure was measured in situ at 7 K by using the T_c shift of the led container.

B. Determination of the temperature dependence of λ from Meissner fraction measurements

The temperature dependence of λ^{-2} was extracted from the Meissner fraction f deduced from low-field

(0.5 mT FC) magnetization data using the relation:²⁵

$$f(T) = \left(\frac{H}{M(T)} - N \right)^{-1}, \quad (14)$$

where H denotes the external magnetic field and N is the demagnetization factor. $N = 1/3$ was taken assuming that the sample grains are spherical. Fig. 1 shows the temperature dependence of the Meissner fraction close to T_c for different pressures. Three important features emerge: (i) The transition temperature T_c increases with increasing pressure. The value of $dT_c/dp = 0.59$ K/kbar is found, which is in good agreement with the literature data.^{14,15,16} (ii) The value of f (Fig. 1) is much smaller than 1, confirming that the average grain size of the sample is compatible with λ . The reduction of f is caused by the field penetration at the surface of each individual grain for distances of the order of λ .²⁶ (iii) The absolute value of the Meissner fraction increases with pressure. Since the average grain size does not change under pressure and the grains are decoupled from each other, the rise of f must be attributed to a decrease of the magnetic penetration depth λ .

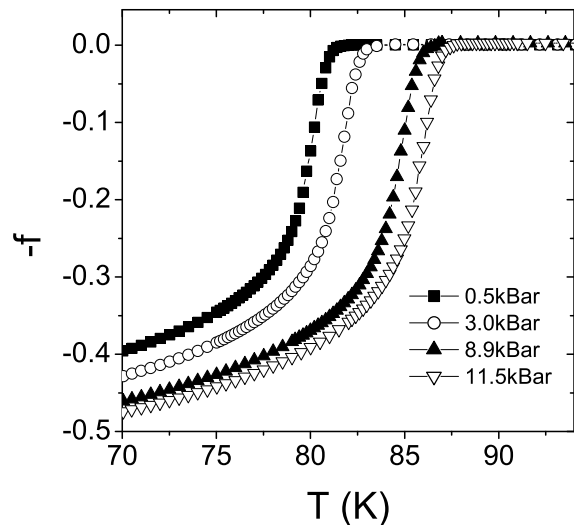


FIG. 1: The temperature dependence of the Meissner fraction f obtained from low-field (0.5 mT, FC) magnetization measurements for various pressures.

The temperature dependence of λ was analyzed on the basis of model suggested by Shoenberg.²⁷ According to Ref. [27] the temperature dependence of the Meissner fraction is given by

$$f(T) = 1 - 3 \left(\frac{\lambda(T)}{R} \right) \coth \left(\frac{R}{\lambda(T)} \right) + 3 \left(\frac{\lambda(T)}{R} \right)^2, \quad (15)$$

where $2R$ is the average grain diameter. By solving this nonlinear equation, λ for each value of f was extracted, and with that the whole temperature dependencies of

λ was reconstructed. Since the sample consists of an anisotropic non-oriented powder, the extracted λ is the so called effective penetration depth λ_{eff} (powder average). However, for sufficiently anisotropic extreme type II superconductors, including $\text{YBa}_2\text{Cu}_4\text{O}_8$, λ_{eff} is proportional to the in-plane penetration depth in terms of $\lambda_{eff} = 1.31\lambda_{ab}$.²⁸ The resulting temperature dependencies of λ_{ab}^{-2} evaluated at different pressures are depicted in Fig. 2. Due to the unknown average grain size the data in Fig. 2 are normalized to the $\lambda_{ab}^{-2}(0)$, taken from μSR measurements.²⁹ The solid lines indicate the leading critical behavior of $\lambda_{ab}^{-2}(T)$ for homogenous and infinite domains

$$\lambda_{ab}^{-2}(T) = \lambda_{0ab}^{-2}|t|^\nu, \quad \nu = 2/3 \quad (16)$$

This equation is a consequence of Eqs. (1) and (6) with critical amplitude

$$\lambda_{0ab}^{-2} = \frac{16\pi^3 k_B T_c}{\Phi_0^2 \xi_{0ab}^t}. \quad (17)$$

The values of λ_{0ab} and T_c obtained from the fit of Eq. (16) to the experimental data presented in Fig. 2 are summarized in Table I. Since Eq. (16) is valid in the vicinity of T_c only, we restricted the fit to the interval from T_c to $T_c - 3$ K.

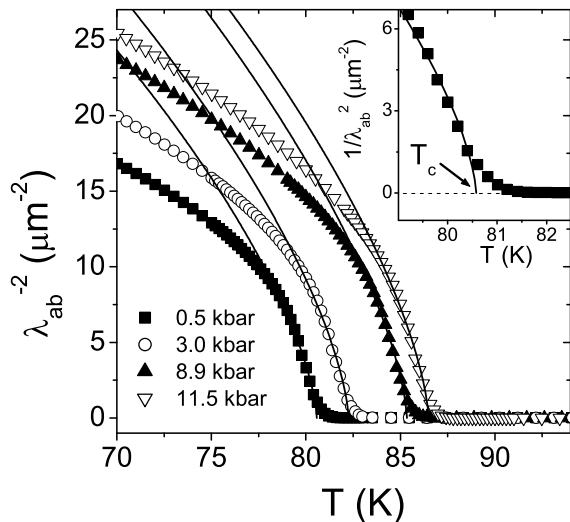


FIG. 2: The temperature dependence of λ_{ab}^{-2} for various pressures obtained from $f(T)$ data (see Fig. 1) by using Eq. (15). The solid lines indicate the leading critical behavior of a homogenous bulk system according to Eq. (16) with the parameters listed in Table I. The inset shows $\lambda_{ab}^{-2}(T)$ in the vicinity of T_c for $p = 0.5$ kbar. The deviation of data points from theoretical curves clearly indicates the finite-size behavior of the system.

IV. THE FINITE-SIZE ANALYSIS

The essential characteristic of a homogeneous bulk cuprate superconductor is a sharp superconductor to normal state transition. A glance to the inset of Fig. 2 shows that in the samples considered here that is not the case. The transition occurs smoothly and there is a tail pointing to a finite-size effect associated with an inflection point at some characteristic temperature T_p . As outlined above [Eq. (3)] at T_p the transverse correlation length ξ_{ab}^t attains the limiting length along the c -axis. To substantiate the occurrence of an inflection point we show in Fig. 3 $d\lambda_{ab}^{-2}(T)/dT$ versus T for $\text{YBa}_2\text{Cu}_4\text{O}_8$ samples at different pressures. The extreme in the first derivative of $\lambda_{ab}^{-2}(T)$ clearly reveals the existence of an inflection point at $T_{pc} < T_c$. The absolute values of T_{pc} obtained from a parabolic fit to experimental data around maximum point are summarized in Table I.

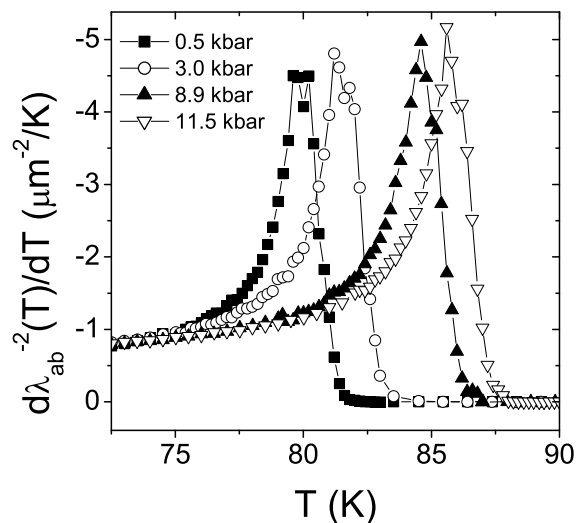


FIG. 3: $d\lambda_{ab}^{-2}(T)/dT$ vs. T at different pressures. The maximum of $d\lambda_{ab}^{-2}(T)/dT$ is at a $T = T_{pc}$.

To substantiate the finite-size scenario further, we explore the scaling properties of the data with respect to the consistency with the finite-size scaling function. Noting that, $\lambda_a \simeq \lambda_b$ and $\nu \simeq 2/3$ in the 3D-XY universality class, Eq.(7) can be rewritten as

$$\frac{\lambda_{0ab}^2}{\lambda_{ab}^2} |t|^{-2/3} = g\left(\frac{t}{t_{pc}}\right). \quad (18)$$

Figure 4(a) shows the resulting scaling function. For comparison, we included the limiting behavior of the finite-size scaling function g_∞ [see Eq. (8)] for a homogeneous ($L_c \rightarrow \infty$) system [the solid line in Fig. 4(a)]. As it is seen, there is quite a good agreement between the experimental data and g_∞ function for t/t_{pc} far from 0 (T far from T_c), whereas in the vicinity of 0 ($T \sim T_c$) the data are completely inconsistent with such a step-wise behavior. The experimental data have to diverge

at $t/t_{pc} \rightarrow 0$. As outlined in Sec. II divergence of the scaling function $g(t/|t_{pc}|)$ at $t/t_{pc} \rightarrow 0$ implies that the system is confined by a finite geometry. To strengthen this point we display in Fig. 4(b) the comparison with the leading finite-size behavior $g_c(t \rightarrow 0) = g_{0c}|t/t_{pc}|^{-2/3}$, as it follows from Eq. (9). Noting that the amplitude g_{0c} depends on the shape of the domains and on the boundary conditions,¹³ it is remarkable that the experimental data collapses on two branches. Accordingly, the shape of the domains and the boundary conditions on the interface do not change significantly under applied pressure. The straight line in Fig. 4 (b) corresponds to $g_{0c} \simeq 0.25$. This value is compatible with $g_{0c} \simeq 0.5$ found for $\text{YBa}_2\text{Cu}_3\text{O}_{6.7}$ oriented powder and for $\text{Bi}_2\text{Sr}_2\text{CaCu}_2\text{O}_{8+\delta}$ thin films.¹³ Much larger values, $g_{0c} \approx 1.1 - 1.6$, have been found for $\text{Bi}_2\text{Sr}_2\text{CaCu}_2\text{O}_{8+\delta}$ single crystals¹³ and for $\text{Y}_{1-x}\text{Pr}_x\text{Ba}_2\text{Cu}_3\text{O}_{7-\delta}$ powders with $0.0 \leq x \leq 0.3$.¹¹

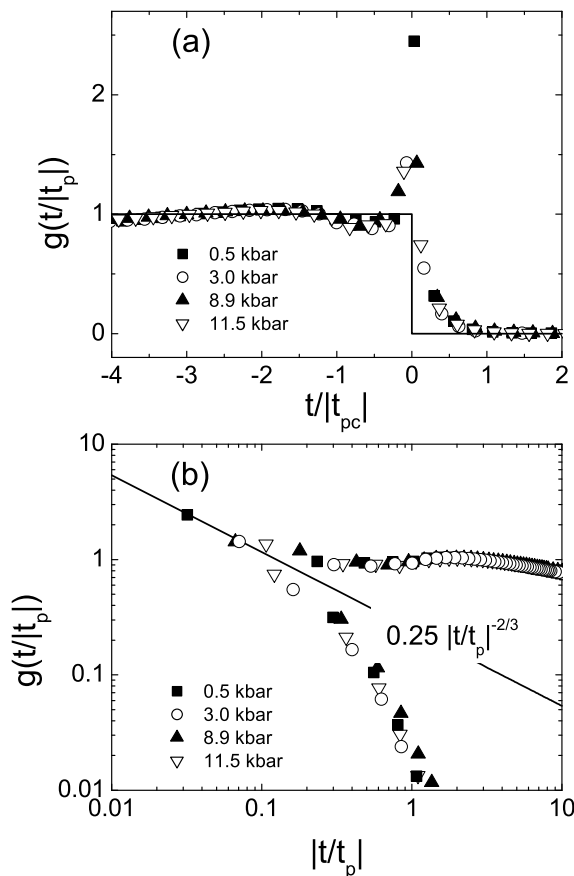


FIG. 4: Finite size scaling function g [Eq. (18)] versus $t/|t_{pc}|$ (a) and versus $|t/t_{pc}|$ in a logarithmic scale (b) for different pressures. The solid stepwise line in (a) is the g_{∞} function for the homogenous ($L_c \rightarrow \infty$) system [see Eq. (8)]. The solid line in (b) is the leading finite-size behavior $g_{0c}|t/t_{pc}|^{-2/3}$ at $t \rightarrow 0$ with $g_{0c} = 0.25$ as it follows from Eq. (9).

To summarize, the finite-size scaling analysis of the in-plane penetration depth data for $\text{YBa}_2\text{Cu}_4\text{O}_8$ is fully

consistent with a finite-size effect. Indeed we established the consistency with all three characteristics of a finite-size effect (see Sec. II). The finite-size estimates for λ_{0ab}^{-2} and $\lambda_{ab}^{-2}(T_{pc})$ at different pressures are summarized in Table I.

V. THE PRESSURE DEPENDENCE OF THE DOMAIN SIZE

Using Eq. (13) and the estimates for T_{pc} and $\lambda_{ab}^{-2}(T_{pc})$ listed in Table I, the domain size L_c along the c -axis is readily calculated. In Fig. 5 we display the pressure dependence of L_c , $T_c(p)$ and $T_{pc}(p)$. It is seen that L_c decreases with pressure, whereas $T_c(p)$ and $T_{pc}(p)$ increase almost linearly. On the other hand T_c and T_{pc} increase with decreasing L_c . This agrees with the behavior found in $\text{Y}_{1-x}\text{Pr}_x\text{Ba}_2\text{Cu}_3\text{O}_{7-\delta}$, where T_c and T_{pc} were found to increase with reduced L_c .¹¹ Here T_c and T_{pc} have been reduced by increasing the Pr content x . In this context it is interesting to note that in granular aluminium T_c was found to increase with reduced grain size.³⁰ Another striking feature is the nanoscale magnitude of L_c , even though $\text{YBa}_2\text{Cu}_4\text{O}_8$ is stoichiometric.

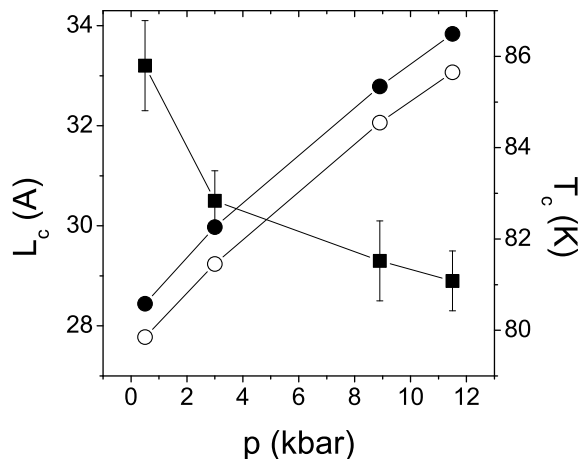


FIG. 5: The pressure dependence of the domain size along the c -axis L_c (■), transition temperature T_c (●), and inflection temperature T_{pc} (○) in $\text{YBa}_2\text{Cu}_4\text{O}_8$.

To check the consistency of our estimates we plot in Fig. 6 the relative shifts of T_{pc} , $\lambda_{ab}^2(T_{pc})$ and L_c versus the relative shift of T_c . According to Eq.(10) these shifts are not independent but related by

$$\frac{\Delta L_c}{L_c} = \frac{\Delta T_{pc}}{T_{pc}} - \frac{\Delta \lambda_{ab}^{-2}(T_{pc})}{\lambda_{ab}^{-2}(T_{pc})}. \quad (19)$$

The straight lines correspond to the linear fits with $\Delta L_c/L_c = -2.18(26) \cdot \Delta T_c/T_c$, $\Delta T_{pc}/T_{pc} = 0.99(1) \cdot \Delta T_c/T_c$ and $\Delta \lambda_{ab}^{-2}(T_{pc})/\lambda_{ab}^{-2}(T_{pc}) = 3.34(27) \cdot \Delta T_c/T_c$, revealing that Eq. (19) is well satisfied. Furthermore,

TABLE I: Finite size estimates for T_{p_c} , λ_{0ab}^{-2} , $\lambda_{ab}^{-2}(T_{p_c})$ and the resulting relative shifts $\Delta T_{p_c}/T_{p_c}$ and $\Delta\lambda_{ab}^{-2}(T_{p_c})/\lambda_{ab}^{-2}(T_{p_c})$ for different pressures. L_{p_c} and $\Delta L_{p_c}/L_{p_c}$ are deduced from Eq.(13).

	T_c	T_{p_c}	λ_{0ab}^{-2}	$\lambda_{ab}^{-2}(T_{p_c})$	L_c	$\frac{\Delta T_c}{T_c}$	$\frac{\Delta T_{p_c}}{T_{p_c}}$	$\frac{\Delta\lambda_{ab}^{-2}(T_{p_c})}{\lambda_{ab}^{-2}(T_{p_c})}$	$\frac{\Delta L_c}{L_c}$
	(K)	(K)	(μm^{-2})	(μm^{-2})	(\AA)	(%)	(%)	(%)	(%)
0.5 kbar	80.58(4)	79.85(3)	93.8(1.5)	3.85(12)	33.2(9)	-	-	-	-
3.0 kbar	82.26(3)	81.45(3)	100.6(1.5)	4.29(11)	30.5(6)	2.08(6)	2.00(5)	11.3(3.7)	-8.2(3.7)
8.9 kbar	85.34(3)	84.55(3)	108.0(1.4)	4.60(13)	29.3(8)	5.91(6)	5.89(5)	19.7(4.0)	-11.7(4.0)
11.5 kbar	86.49(3)	85.65(3)	109.8(1.5)	4.74(13)	28.9(6)	7.33(6)	7.26(5)	23.3(3.8)	-12.8(3.7)

these estimates show that the reduction of L_c with pressure reflects the fact that the pressure effect on $\lambda_{ab}^{-2}(T_{p_c})$ exceeds the effect on T_c considerably. Having established the consistency of our estimates it is essential to recognize that the occurrence of nanoscale superconducting domains is not an artefact of $\text{YBa}_2\text{Cu}_4\text{O}_8$ and our samples. Indeed the existence of nanoscale domains has been established in a variety of cuprates, including films, powders and single crystals.¹³

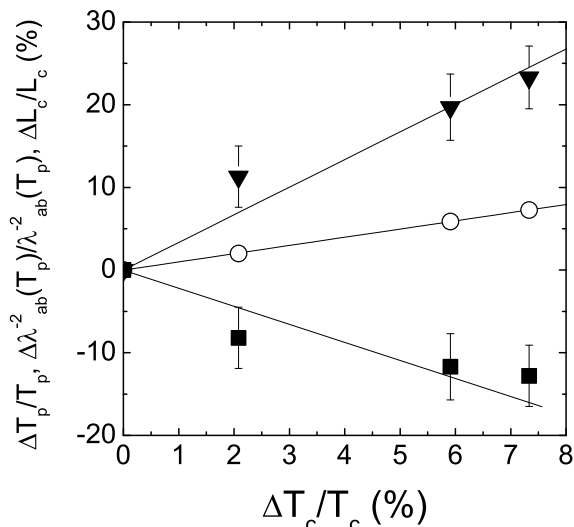


FIG. 6: The relative shifts of $\Delta\lambda_{ab}^{-2}(T_{p_c})/\lambda_{ab}^{-2}(T_{p_c})$ (\blacktriangledown); $\Delta L_c/L_c$ (\blacksquare), and $\Delta T_{p_c}/T_{p_c}$ (\circ) vs the relative shift of $\Delta T_c/T_c$. The solid lines represent the linear fits with $\Delta L_c/L_c = -2.18(26) \cdot \Delta T_c/T_c$, $\Delta T_{p_c}/T_{p_c} = 0.99(1) \cdot \Delta T_c/T_c$ and $\Delta\lambda_{ab}^{-2}(T_{p_c})/\lambda_{ab}^{-2}(T_{p_c}) = 3.34(27) \cdot \Delta T_c/T_c$.

VI. CONCLUSION

To summarize, we report the first observation of combined finite-size and pressure effects on the lengths L_c

of the superconducting domains along the c -axis and the in-plane penetration depth λ_{ab} in a cuprate superconductor. The evidence for a finite-size behavior of the system arises from the tail in $\lambda_{ab}^{-2}(T)$ observed in the vicinity of T_c . We have shown that the scaling properties of the tail are fully consistent with a finite-size effect, arising from domains with nanoscale size along the c -axis. Indeed the essential characteristics of a finite-size effect, as (i) the limiting properties of the scaling function $g(t/|t_{p_c}|)$, (ii) the existence of an inflection point in $\lambda^{-2}(T)$ and (iii) the extremum in $d\lambda^{-2}(T)/dT$ at T_{p_c} have been verified. Even though $\text{YBa}_2\text{Cu}_4\text{O}_8$ is *stoichiometric* we have shown that the size of the domains along the c -axis is of nanoscale only, ranging from 33.2 \AA to 28.9 \AA at pressures from 0.5 to 11.5 kbar. This raises serious doubts on the existence of macroscopic phase coherent superconductivity. Contrariwise this does not exclude a percolative resistive superconductor to normal state transition, when the superconducting domains percolate. Indeed, a granular superconductor is usually characterized by two parameters:³¹ the first is the domain's size and the second the coupling between them. The coupling is accomplished randomly with a temperature dependent probability. Such a mechanism is a percolation process; at the temperature where the coupling probability is equal to the percolation threshold, an infinite cluster of coupled superconducting grains is formed. This suggests that resistive bulk superconductivity is achieved by a percolative process, while the phase coherent superconducting properties and the spatial extent of the domains can be probed by thermal fluctuations and finite-size effects.

The authors are grateful to J. Roos for stimulating discussions, K. Conder for help during sample preparation and T. Strässle for providing pressure cell for magnetization measurements. This work was supported by the Swiss National Science Foundation and by the NCCR program *Materials with Novel Electronic Properties* (MaNEP) sponsored by the Swiss National Science Foundation.

* Electronic address: rustem.khasanov@psi.ch; Current address: *Laboratory for Neutron Scattering, ETH Zürich and*

Paul Scherrer Institut, CH-5232 Villigen PSI, Switzerland;

- DPMC, Université de Genève, 24 Quai Ernest-Ansermet, 1211 Genève 4, Switzerland; Physik-Institut der Universität Zürich, Winterthurerstrasse 190, CH-8057, Switzerland
- ¹ G. Bednorz and K. A. Müller, Z. Phys. B **64**, 189 (1986).
 - ² J. Mesot, P. Allenspach, U. Staub, A. Furrer, and H. Mutka, Phys. Rev. Lett. **70**, 865 (1993).
 - ³ A. Furrer, P. Allenspach, F. Fauth, M. Guillaume, W. Henggeler, J. Mesot, and S. Rosenkranz, Physica C **235-240**, 261 (1994).
 - ⁴ N. Alekseevskii, I. Garifullin, N. Garif'yanov, B. Kochelaev, A. Mitin, V. Nizhankovskii, L. Tagirov, G. Khaliullin, and E. Khlybov, Sov. JEPT Lett. **48**, 37 (1988).
 - ⁵ J.X. Liu, J.C. Wan, A.M. Goldman, Y.C. Chang, and P.Z. Jiang, Phys. Rev. Lett. **67**, 2195 (1991).
 - ⁶ A. Chang, Z.Y. Rong, Y.M. Ivanchenko, F. Lu, and E.L. Wolf, Phys. Rev. B **46**, 5692 (1992).
 - ⁷ T. Cren, D. Roditchev, W. Sacks, J. Klein, J.-B. Moussy, C. Deville-Cavellin, and M. Laguës, Phys. Rev. Lett. **84**, 147 (2000).
 - ⁸ K.M. Lang, V. Madhavan, J.E. Hoffman, E.W. Hudson, H. Eisaki, S. Uchida, and J.C. Davis, Nature (London) **415**, 412 (2002).
 - ⁹ D. Di Castro, G. Bianconi, M. Colapietro, A. Pifferi, N. L. Saini, S. Agrestini, and A. Bianconi, Eur. Phys. J. B **18**, 617 (2000).
 - ¹⁰ T. Schneider, cond-mat/0210702.
 - ¹¹ T. Schneider, R. Khasanov, K. Conder, and H. Keller, J. Phys.: Cond. Matt. **15**, L763 (2003).
 - ¹² T. Schneider, J. Superconductivity **17**, 41 (2003).
 - ¹³ T. Schneider and D. Di Castro, Phys. Rev. B **69**, 024502 (2003).
 - ¹⁴ J.J. Scholtz, E. N. van Eenige, R. J. Wijngaarden, and R. Griessen, Phys. Rev. B **45**, 3077 (1992).
 - ¹⁵ B. Bucher, J. Karpinski, E. Kaldis, and P. Wachter, Physica C **157**, 478 (1989).
 - ¹⁶ E.N. van Eenige R. Griessen, R.J. Wijngaarden, J. Karpinski, E. Kaldis, S. Rusiecki, and E. Jilek, Physica C **168**, 482 (1990).
 - ¹⁷ Shang-Keng Ma in: *Modern Theory of Critical Phenomena*, Frontiers in Physics **46** (W.A. Benjamin, Inc., Reading, Massachusetts, 1976).
 - ¹⁸ T. Schneider and J. M. Singer, *Phase Transition Approach To High Temperature Superconductivity*, Imperial College Press, London, 2000.
 - ¹⁹ P. C. Hohenberg, A. Aharony, B.I. Halperin, and E.D. Siggia, Phys. Rev. B **13**, 2986 (1976).
 - ²⁰ M.E. Fisher and M.N. Barber, Phys. Rev. Lett. **28**, 1516 (1972).
 - ²¹ J.L. Cardy ed., *Finite-Size Scaling*, North Holland, Amsterdam 1988.
 - ²² N. Schultka and E. Manousakis, Phys. Rev. B **13**, 2986 (1976).
 - ²³ T. Schneider, J. Hofer, M. Willemin, J. M. Singer, and H. Keller, Eur. Phys. J. B **3**, 413 (1998).
 - ²⁴ T. Strässle, Ph.D. thesis, ETH Zürich, 2002.
 - ²⁵ S. Blundell *Magnetism in Condensed Matter* (Oxford university press, Oxford, 2001).
 - ²⁶ G.M. Zhao M.B. Hunt, H. Keller, and K.A. Müller, Nature (London) **385**, 236 (1997).
 - ²⁷ D. Shoenberg, Proc. R. Soc. Lond. **A 175**, 49 (1940).
 - ²⁸ V.I. Fesenko, V.N. Gorbunov, and V.P. Smilga, Physica C **176**, 551 (1991).
 - ²⁹ R. Khasanov, D. Di Castro, D.G. Eshchenko, D. Andreica, K. Conder, S. Kazakov, J. Karpinski, E. Pomjakushina, I.M. Savić, R. Tetean, and H. Keller, in preparation.
 - ³⁰ G. Deutscher *et al.*, J. Low. Temp. Phys. **10**, 231 (1973).
 - ³¹ G. Deutscher, O. Entin-Wohlman, S. Fishman, and Y. Shapira, Phys. Rev. B **21**, 5041 (1980).